Contents lists available at ScienceDirect

Nuclear Instruments and Methods in Physics Research A

journal homepage: www.elsevier.com/locate/nima

Liquid helium-free cryostat and hermetically sealed cryogenic microwave cavity for hyperfine spectroscopy of antiprotonic helium

O. Massiczek *, S. Friedreich, B. Juhász, E. Widmann, J. Zmeskal

Stefan Meyer Institute for Subatomic Physics, Austrian Academy of Sciences, Boltzmanngasse 3, 1090 Vienna, Austria

ARTICLE INFO

ABSTRACT

The design and properties of a new cryogenic set-up for laser–microwave–laser hyperfine structure spectroscopy of antiprotonic helium – an experiment performed at the CERN-Antiproton Decelerator (AD), Geneva, Switzerland – are described. Similar experiments for ^{4}He have been performed at the AD for several years. Due to the usage of a liquid helium operated cryostat and therefore necessary refilling of coolants, a loss of up to 10% beamtime occurred. The decision was made to change the cooling system to a closed-circuit cryocooler. New hermetically sealed target cells with minimised ^{3}He gas volume and different dimensions of the microwave resonator for measuring the ^{3}He transitions were needed. A new set-up has been designed and tested at Stefan Meyer Institute in Vienna before being used for the 2009 and 2010 beamtimes at the AD.

© 2011 Elsevier B.V. Open access under CC BY-NC-ND license.

1. Introduction

Antiprotonic helium ($\overline{p}He^+$) is a metastable three body system composed of a He nucleus, an electron and an antiproton ($\overline{p}$). Due to its relatively long lifetime (several μs) it can be used for studies on the antiproton magnetic moment. The experimental method is called laser–microwave–laser spectroscopy [1–4]: 3.5 GeV/c $\overline{p}$ are produced by pair production (26 GeV/c protons hitting an iridium target) and injected into the CERN[1] Antiproton Decelerator (AD [5]). After deceleration to 100 MeV/c the $\overline{p}$ are ejected to the experimental gas target where $\overline{p}He^+$ is formed by replacing one of the e$^-$ in the He atoms by a $\overline{p}$. Some 3% of these exotic atoms remain in metastable states which can be used to determine the $\overline{p}$ magnetic moment by measuring microwave induced population transfers within the hyperfine structure. To obtain a signal, two laser pulses are applied, one before, another one after the microwave pulse. The laser pulses induce a depopulation by transfer to a fast decaying state, which can be detected by observing time spectra of the Cherenkov light produced by the decay products (mostly pions) passing through the Cherenkov counters. These detectors are placed as close as possible to the experimental target to maximise the solid angle.

To resolve the hyperfine dublet structure of the $\overline{p}He^+$ transitions, with a splitting of 1.72 GHz in ^{3}He, cryogenic conditions are required during the experiment to reduce Doppler broadening which is the main cause of line broadening in this experiment. Therefore, the temperature of the experimental gas must be well below 10 K. A temperature of about 6.2 K was easily achievable without too big efforts. The resulting Doppler broadening of about 425 MHz (^{3}He) has shown to be sufficiently small to be able to separate the hyperfine lines [2]. The dependence of Doppler broadening v_D on mass (M) and temperature (T) – with k being the Boltzmann constant and c being the speed of light – is as follows:

$$\Delta v_D = 2.35 v \sqrt{\frac{kT}{Mc^2}} \tag{1}$$

The cryostat used in previous experiments with ^{4}He was a combined liquid helium (ℓHe) and liquid Nitrogen (ℓN_2) operated one (described in Ref. [6]).

Due to necessary refilling of ℓHe during the 8–12 h shifts, a loss of up to 10% beamtime occurred. To avoid beamtime losses and because of the necessity for a new microwave set-up for measurements with ^{3}He, which would not have fit into the existing cryostat, a new – ℓHe-free – cryocooler-based cryostat was designed.

The technical details of the composition of the cryostat (Section 2), the target cells (Section 3), the vacuum chamber (Section 4), the magnetic shielding around the set-up (Section 5) and the gas system (Section 6) will be described in this paper as

---

* Corresponding author. Tel.: +43 1 4277 29725; fax: +43 1 4277 9297.
  E-mail addresses: oswald.massiczek@cern.ch,
oswald.massiczek@oeaw.ac.at (O. Massiczek).
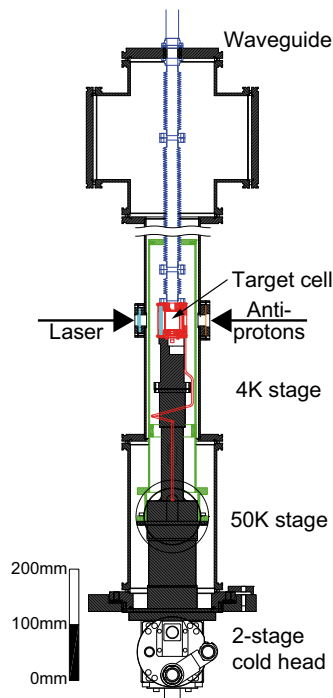 [1] European Organisation for Nuclear Research, Geneva, Switzerland

Fig. 1. Vertical sectional drawing of the new cryostat (drawing shortened between wavy horizontal lines). A detailed drawing of the target cell area is shown in Fig. 3.

well as the behaviour of the temperature control (Section 7) and problems (Section 8) experienced during the experimental runs.

2. Cryostat

The cryostat, shown in Fig. 1, is based on a two-stage Gifford–McMahon cryocooler[2] that has 50 W cooling power of the first stage at 36.4 K, while the second stage is absorbing 1 W at 4.01 K temperature. The first stage is attached to a thermal radiation shield that reduces the heat load to the target cell. The radiation shield is made of a square aluminium tube with 80 mm inner side, 2 mm wall thickness, and 452 mm height. The shield was bolted to an adaptor attached to the first stage of the cryocooler. Two holes of 20 mm diameter were machined in the shield walls for the access of the antiproton and laser beams. Small clearances were cut onto the shield for the waveguide, the target gas pipe, and the instrument wires, taking care of minimal direct leakage of room temperature radiation onto the target cell. The shield was finally wrapped with multilayer insulation (MLI) that left the beam access holes uncovered. The shield temperature varied between 45 and 50 K during the experimental runs, depending on the target cell and gas pressure. Some details of the shield are shown in Figs. 2 and 3. Two waveguides were used in order to cover the required frequency range, WR75 for frequencies between 10 and 15 GHz, and WR62 for frequencies between 12.4 and 18 GHz. Seamless flexible brass waveguides[3] were used, in order to compensate the thermal dilatation upon cooldown, and to minimise the heat loads to the shield and to the cell due to the thermal bridges made by the guides. The guides were wrapped in MLI and the guide lengths used all 908 mm length available from the feed through on the top flange down to the target cell.
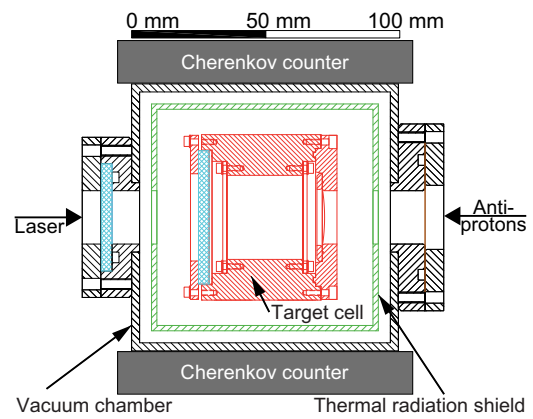
Fig. 2. Horizontal sectional drawing of the target cell area (version A). Laser is coming from the left, antiprotons from the right.
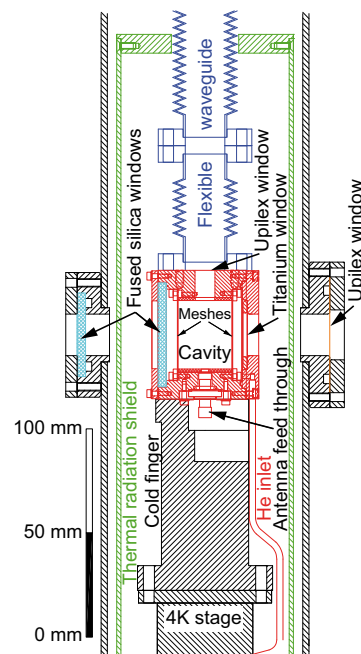

Fig. 3. Target cell layout (version B, enlarged centre part from Fig. 1), connected to cold finger below and flexible waveguide above. Laser is coming from the left, antiprotons from the right.

3. Target cells

3.1. Requirements

The design of the target cell had to fulfil a certain set of requirements: three different cylindrical microwave cavities at operation frequencies of 11.14 GHz (^{3}He), 12.93 GHz (^{4}He) and 16.13 GHz (^{3}He) needed to be built into hermetically sealed cryogenic targets (one cavity per cell). These cavities had to be suitable for the TM_{110} mode (i.e. approximately constant field along the z-axis). This mode was chosen due to the cylindrical shape of the overlap volume of the stopping distribution of the antiprotons with the laser beam. The cavity sizes ranged from around 11 to 18 mm in radius and 18 to 26 mm in length. Each target cell had to be equipped with three windows (for antiprotons, laser, microwaves), one feed through (microwave pickup antenna) and an inlet for the helium gas used during the experiment. Also the size of the cell had to be matched to the stopping distribution of the antiprotons [6] to fit inside the microwave

cavity. The connection between the target cells and the cold head was established by a transition piece (cold finger) made from oxygen-free high-conductivity copper. All this had to fit into the space confined by the thermal radiation shield having an inner spacing of $(8 \text{ cm}) \times (8 \text{ cm})$ in the horizontal plane (see Fig. 2). This space was delimited by the need to maximise the solid angle with respect to the Cherenkov counters outside the vacuum chamber.

3.2. Solutions

The following solutions were found to fulfil the requirements for the target cell windows and feed throughs:

- Laser entrance window: fused silica[4], diameter 50 mm, thickness 4 mm, uncoated – indium sealed.
- $\bar{p}$ Entrance window: 25 µm Ti-foil[5] glued into a brass mounting – indium sealed.
- Helium gas inlet: 2 mm hole in the mounting ring of the $\bar{p}$ window with glued-in pipe (outer diameter: 3 mm, wall thickness: 0.5 mm, material: stainless steel) and hose[6] as connection to the outside.
- a waveguide for feeding the microwaves into the cavity, connected by a pressure window: 50 µm polyimide film[7] – indium sealed.
- an antenna feed through: Cryogenic both-sided SMA plug, 50 Ω[8] and coaxial cable for the microwave pickup antenna – indium sealed.
- stainless steel meshes (see Section 3.5) for confining the microwaves in a defined volume of the experimental target cell.

All glueing was done with a two component epoxy adhesive,[9] the indium wires for sealing were 1 or 1.5 mm thick and inserted into fitting grooves.

A technical drawing can be seen in Fig. 3.

3.3. Material choice

After trying different materials such as stainless steel (too low thermal conductivity for this kind of set-up) and copper (too soft for precise machining), the material chosen for the type A version of the target cell was brass, which has proven to be the optimum combination of machinability and thermal conductivity. As an improvement in the type B version a stainless steel tube with a wall thickness (only related to ease of machining, not to the frequency) of 1.78 mm (11 GHz) or 1.56 mm (13 GHz), respectively, was placed inside the target cell acting as a microwave cavity (work on the 16 GHz version is in progress) in order to be able to define the microwave properties more precisely without having to remachine the cryogenic target cell itself. This caused a slightly higher temperature offset between the sensor placed on the exterior of the target cell and the actual gas temperature compared to the purely brass made cavity (see also Section 7 and Fig. 6).

3.4. Interchangeability

To make as many parts as possible interchangeable between the target cells, the dimensions of the windows and feed throughs were desired to be the same for all microwave cavities. Due to size limitations this was not entirely possible for the 16 GHz cavity.

3.5. Meshes

For confining the microwaves in the horizontal cylindrical cavity part of the target cell, the faces of the cavity were covered by two stainless steel (316L) meshes (transmissibility $> 90\%$, 250 µm thick, wire thickness 0.05 mm, wire clearance 0.75 mm, made by electric discharge machining), still allowing the laser and the antiprotons to enter. The first version made from thinner material by techniques of photo-etching a 50 µm copper foil has proven to be too soft and therefore wobbly, possibly causing an unwanted deterioration of the microwave resonator shape.

3.6. Impurities

The problem of brass is normally its high outgasing rate into vacuum. This was not an issue relevant to this experiment, as the set-up is operated at a very low temperature (< 10 K) and therefore everything apart from the helium experimental gas freezes out at some point during the cooldown process – the additional outgassing from the brass part into the insulation vacuum was too small to be measurable at all.

4. Vacuum chamber

Around the cryogenic part of the set-up, a vacuum chamber was designed, mostly out of commercially available standard ISO-K (1 DN 160 crosspiece, 1 DN 160/DN100 crosspiece, 1 DN 100 measurement crosspiece, adaptor pieces to ISO-KF) and ISO-KF (feed throughs, blind flanges) vacuum parts. Nevertheless, three main parts had to be custom made: the vacuum chamber around the target area, which needed to be square shaped to provide an optimum solid angle for the Cherenkov detectors (acrylic scintillators attached to gated PMTs – described in Ref. [7]), the top feed through for the waveguide and the pivotable adaptor flange for mounting the cold head on the lower end of the cryostat.

Three windows had to be built into the vacuum chamber:

- Laser window: fused silica[10], diameter 40 mm, thickness 4 mm, uncoated (O-ring seal).
- Antiproton window: 50 µm polyimide film[11] (O-ring seal).
- Microwave waveguide pressure window[12] made from teflon (O-ring seal), replaced by a custom made Indium sealed 50 µm polyimide film[13]-window later on – see also Section 8.

Additionally, the following feed throughs from insulation vacuum to the outside were needed (all of them situated in the lower part of the vacuum chamber):

- SMA-microwave antenna cable feed through[14] electron-beam welded into an ISO-KF-50 blind flange,
- 8-pin feed through for cavity and cold finger temperature sensors (ISO-KF-16),
- 9-pin feed through (4 pins used) for heater and Pt100 thermal shield temperature sensor (ISO-KF-40),
- helium gas feed through (outer diameter: 8 mm, wall thickness: 1 mm stainless steel pipe with VCR connectors on both ends welded into an ISO-KF-40 blind flange).

---

[4] Edmund Optics N-BK7.
[5] Advent Research Materials Ltd.
[6] Swagelok 321-4-X-12FR.
[7] Upilex foil made by UBE Industries.
[8] Vacom W-SMA50-SH-DE-CE-INC.
[9] Hysol EA 9361.

[10] Edmund Optics N-BK7.
[11] Upilex foil made by UBE Industries.
[12] The Waveguide Solution, RW17-SZB-412-402-B.
[13] Upilex foil made by UBE Industries.
[14] Similar to Vacom W-SMA50-SH-DE-CE-INC.

Other vacuum parts used were (both located towards the top end of the vacuum chamber):

- vacuum to air (or pure N_2) valve (ISO-KF-16),
- pressure gauge[15] (ISO-KF-25).

For pumping the insulation vacuum, a turbomolecular pump[16] has been chosen. Combined with a scroll pump as roughing pump, the best achievable insulation vacuum revealed to be in the low 10^{-7} mbar range.

5. Mu-metal magnetic shielding

The linewidth of the microwave transitions increases by 2.8 MHz/G in the presence of a constant magnetic field. The field in the target volume has to be < 0.1 G to ensure that the broadening is smaller than the natural linewidth (about 2 MHz for the 11 GHz transitions in ^{3}He). Therefore a 1 mm thick Mu-metal shielding was designed around the square shaped part of the vacuum chamber, reaching from about 20 cm below up to about 40 cm above the target cell position, to minimise the influence of external magnetic fields in the target area. As a result, the maximum magnetic field strength measured at the target cell position inside the magnetic shielding was sufficiently small – below 0.05 G compared to 0.6 G without magnetic shielding (caused by the earth magnetic field). The first measurements of the magnetic fields were done at SMI[17] with a gauss-meter,[18] using axial and transverse Hall probes. Later on measurements at the AD showed that stray magnetic fields (e.g. from beamline steering magnets) inside the experimental area did not cause a different result.

6. Gas system

Outside the cryostat a gas system (a schematic drawing can be seen in Fig. 4) had to be developed for the following tasks:

- cleaning the experimental ^{3}He gas from chemical impurities before filling the target cell,
- recuperating the used ^{3}He in order to avoid losing this expensive gas,
- avoiding overpressure in the experimental set-up by relieving it without losing ^{3}He.

For cleaning purpose, a liquid nitrogen operated cold trap filled with 13X/4A molecular sieve (6 mm outer diameter, 1 mm wall thickness soft copper pipe – with one in-line particulate filter[19] attached to each end – bent to a coil fitting into a 2 l ℓN_2-dewar) was installed in the system. The recuperation system consists of two pumps, leading the helium back into its original bottle and pressurising it up to 3 bar. For safety reasons, an overpressure valve opening at 1.8 bar venting the gas into an 1 U.S. Gal. (approx. 3.8 l) expansion bottle had to be installed. With this valve installed, an uncontrolled warmup of the system puts no risk on the set-up as the weakest part of the gas system (the titanium window of the target cell) can withstand > 4 bar, so the expansion of the gas into the expansion volume starting from 1.8 bar pressure inside the target cell results in a sufficiently large
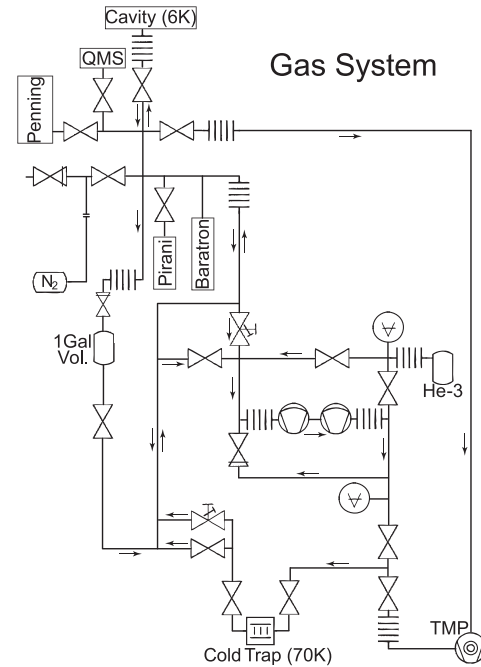

Fig. 4. Schematic drawing of the gas system, all components at room temperature (if not marked different). Symbols according to DIN 28401.

safety margin with regards to the relatively low overpressures used in this experimental set-up. Most parts of the gas system were designed using Swagelok parts: flexible tubes, valves, needle valves, pressure relief valves with VCR-fittings (a proprietary, highly reliable, washer-based, all metal sealing system). Only in a few places standard Swagelok all metal tube fittings had to be used due to very special design requirements (e.g. connection to the cold trap, connection to the gas bottle's reduction valve). Also adapters to other connection types were needed, such as a VCR to NPT connectors for use with the expansion bottle and VCR to ConFlat and ISO-KF adapters as a connection to a remaining part of the old gas system – including Baratron, Penning and Pirani pressure gauges and a Q-mass spectrometer – which was continued to be used.

7. Temperature control

The temperature behaviour of the new cryostat was recorded by reading out three temperature sensors, thereof two silicon diodes,[20] one screwed on top of the target cell, the other onto one side of the cold finger. Those sensors were read out by an auto-tuning temperature controller.[21] The third sensor, a Pt100 (platinum sensor) in a two-wire configuration was glued onto the inside of the top cover of the thermal radiation shield and read out by a digital voltmeter.

7.1. Temperature stabilisation

For controlling the temperature, two heating resistors ($2 \times 10\ \Omega$) were screwed on the cold finger between the cold head and the target cell. The temperature sensor mounted on top of the target cell was used by the temperature controller as a

---

[15] Balzers compact full range PKR 250.
[16] Varian Turbo-V 301, air cooled.
[17] Stefan Meyer Institute.
[18] LakeShore 421.
[19] Swagelok SS-6F-MM-2.

[20] LakeShore Cryotronics Inc. DT-670, CU packaged.
[21] LakeShore 331S.

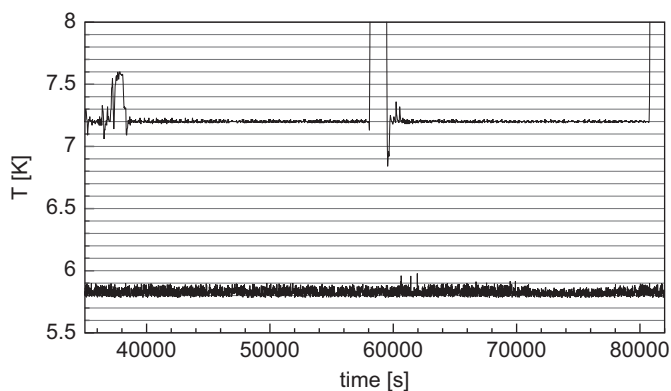**Fig. 5.** Temperature stability nearby the cavity. Upper curve: old ℓHe cooled cryostat – 7.2 K shown by the sensor corresponds to 6.2 K in the target volume, the huge temperature excursions are caused by periodic refilling of coolants. Lower curve: compressor-operated cryostat – 5.8 K shown by the sensor corresponds to 6.2 K in the target volume.

Fig. 6. Liquid helium calibration curves (broken lines) of different cavity versions (i.e. the target cell type A and two of the target cells type B) compared to the vapour pressure curve of ℓHe (continuous line), thus showing the offset in temperature between the temperature read from the sensor and the actual temperature of the experimental gas inside the cavity.

control loop stabilising the temperature together with the two heaters.

The amplitude of the temperature fluctuations on the sensor has shown to be bigger than in the old cryostat but still sufficiently small (a comparison can be seen from Fig. 5) – the oscillation amplitude was depending on the target cell installed and the pressure inside. The main advantage of the new set-up was the avoidance of any large-scale temperature changes (and therefore unnecessary risks such as leaks or overpressures) which occurred during refilling of the cryocoolants in the old cryostat.

7.2. Temperature calibration

A minimum temperature of around 4.8 K was achieved inside the target cell during the calibration process conducted with liquid helium (at a vapour pressure of 1600 mbar). This calibration process was necessary to determine the temperature offset between the value shown by the temperature sensor mounted on the outside of the cavity and the actual He gas temperature. The offset has been in the range between 0.2 and 0.4 K (see Fig. 6).

7.3. Cooldown and warmup

The cooldown time of the set-up needs to be short as swapping (i.e. craning in and aligning the set-up, which can only be done at room temperature) from one experiment to another or one target cell to another should take as little time as possible. Cooldown times have shown to be satisfying, i.e. cooldown from room temperature to 8 K can be achieved within 3 h, down to 6 K in another 2 h (see Fig. 7) and for calibration purposes (not needed during the run), cooldown to 4.5 K takes a total time of 12 h. Warmup times have also shown to be compatible with the need to warm up fast enough to be able to change the target cells in a (slightly extended) break between two shifts (i.e. 16–20 h, see Fig. 8).

7.4. Pressure changes

The temperature behaviour during experimentally necessary pressure changes did not cause any problems. The readjustment time of the temperature after pressure changes (see also Fig. 9) was pressure dependent (60–1500 s). In the typical pressure ranges (150–500 mbar) this time was considerably shorter (typically below 5 min) compared to the old cryostat which had much longer time constants (typically 30 min) due to its significantly bigger helium gas volume.
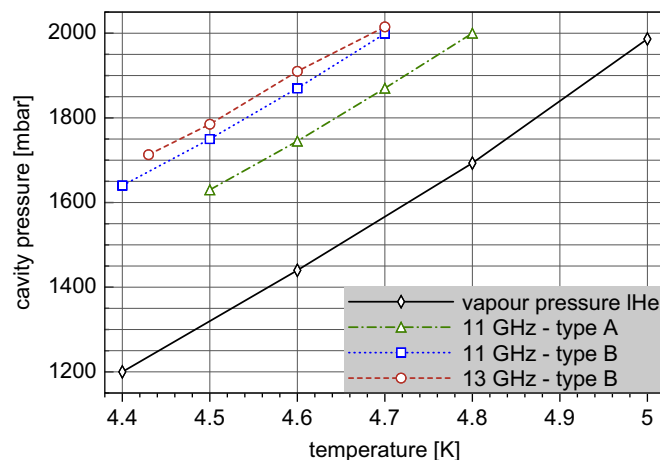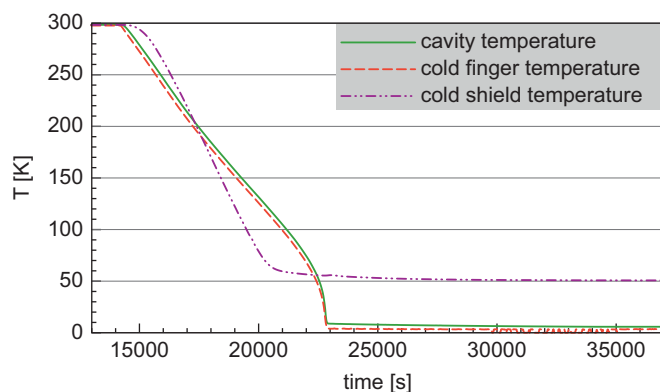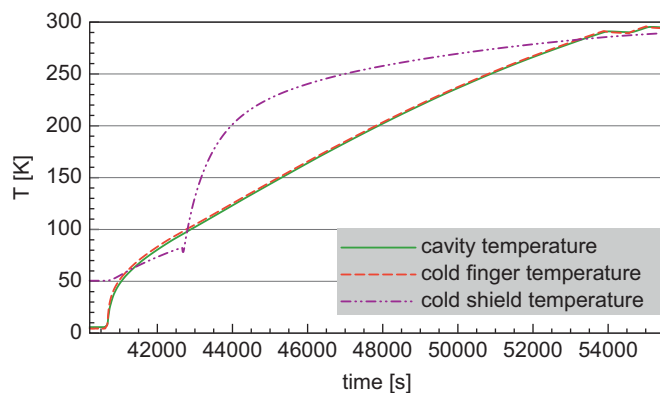

Fig. 7. Cooldown process.

Fig. 8. Warmup process. When the thermal radiation shield temperature reached 80 K, the vacuum chamber was vented with N_2.

8. Problems and solutions

After experiencing some problems with a cold leak of the target cell at around 10^{-4} mbar l/s during the first run (2009) with the new set-up, some little improvements have been made to the design of the groove holding the indium wires for the laser window and for the waveguide connection in place. Those changes to the design of the seals resulted in a smoother performance.
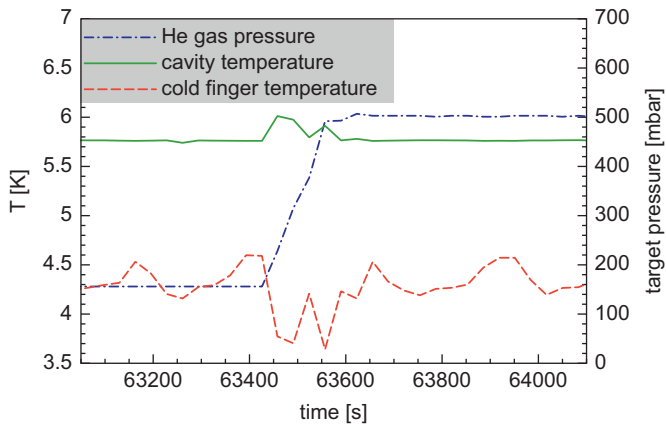
Fig. 9. Temperature and pressure stabilisation within 200 s after start of changing to a higher gas pressure for changing the target gas density.

During the 2010 beamtime, a commercially obtained part (waveguide pressure window mentioned in Section 4) failed and therefore the insulation vacuum broke without damaging other parts of the set-up. It had to be put out of service and was replaced by a self-designed solution, using indium sealed poly-imide film.[22]

9. Summary

We have described the design and behaviour of an ℓHe-free cryostat successfully used for doing hyperfine structure spectroscopy of $\overline{p}^3$He and $\overline{p}^4$He carried out at the CERN-AD. This set-up is based on a two-stage compressor-based cooling system with a hermetically sealed cryogenic experimental target cell attached and built into an insulation vacuum chamber. Indium wires have proven to be the best solution for sealing the windows and feed throughs of the target cell. After some minor problems with the target cell leaking during the 2009 beamtime, the performance during the 2010 beamtime was highly satisfactory.

Acknowledgements

References

[1] E. Widmann, et al., Phys. Rev. Lett. 89 (2002) 243402.
[2] T. Pask, et al., J. Phys. B: At. Mol. Opt. Phys. 41 (2008) 081008 (8pp).
[3] T. Pask, et al., Phys. Lett. B 678 (1) (2009) 55.
[4] S. Friedreich, et al., Spectroscopy of the Hyperfine Structure of Antiprotonic ^{4}He and ^{3}He, Hyperfine Interactions, in print (2011).
[5] S. Baird, et al., Nucl. Phys. B (Proc. Suppl.) 56A (1997) 349.
[6] J. Sakaguchi, et al., Nucl. Instr. and Meth. Phys. Res. A 533 (2004) 598.
[7] M. Hori, et al., Nucl Instr. and Meth. Phys. Res. A 496 (2003) 102.

---

[22] Upilex foil made by UBE Industries.